

Novel Interface-Mediated Metastable Oxide Phases: Vanadium Oxides on Pd(111)

S. Surnev,¹ G. Kresse,² M. G. Ramsey,¹ and F. P. Netzer¹

¹*Institut für Experimentalphysik, Karl-Franzens-Universität Graz, A-8010 Graz, Austria*

²*Institut für Materialphysik, Universität Wien, A-1090, Vienna, Austria*

(Received 1 February 2001; published 2 August 2001)

In the growth process of ultrathin films of vanadium oxides on Pd(111), a sequence of novel oxide phases with layer-dependent structures and oscillating oxidation states has been detected experimentally and understood theoretically. These phases are interface mediated and metastable with respect to further oxide growth. Transformation into the stable oxide configuration occurs beyond a critical thickness, where energetics combined with kinetic limitations determine the oxide multilayer structure.

DOI: 10.1103/PhysRevLett.87.086102

PACS numbers: 68.35.Md, 68.37.Ef, 71.15.Mb, 81.10.-h

Ultrathin films of metal oxides are important materials for solid-state electronic devices, sensors, and for a wide range of catalytic processes [1,2]. They often exhibit novel, nonbulklike properties and structures which originate from spatial confinement and proximity effects to dissimilar materials, such as metals or other metal oxide substrates. In the field of catalysis, an important example is the so-called oxide “monolayer” catalyst, which consists of an ultrathin transition metal oxide film, only one to a few layers thick, supported by another oxide substrate [3,4]. These monolayer oxide catalysts display superior catalytic properties with enhanced activity and selectivity as compared to those encountered by the individual oxide components, but the physical origin of the enhanced reactivity is still unclear.

In the case of transition metal oxides with various oxidation states, such as, e.g., Ti, Cr, or Fe oxides, previous experimental results have indicated that the oxide layers formed directly at the interface to another metal have a lower oxidation state than the thermodynamically most stable phases [5]. This is presumably the result of the reducing character of the metal surface, but a detailed study of this effect is lacking. In this Letter, we report a quasioscillatory behavior of the oxidation states of ultrathin vanadium oxide layers observed using scanning tunneling microscopy (STM), low-energy electron diffraction (LEED), x-ray photoelectron spectroscopy (XPS), and first-principles density functional theory (DFT) calculations, during oxide growth on Pd. These interfacial layers constitute novel oxide phases which are metastable with respect to further oxide growth and transform into the stable bulklike oxide, in this case V_2O_3 , after the films have reached thicknesses of >3 oxide layers.

The physical origin of this layer-dependent evolution of vanadium oxide structures has been investigated by first-principles DFT calculations (including STM simulations) of the various oxide phases and their interfaces. We stress that the intermediate V oxide structures observed here are examples of novel oxide phases, with particular oxidation states and structures, which develop uniquely in the interfacial thin-layer limit. Conceptually, similar oxide phases may be present in ultrathin layers of other supported

oxides as well, with important consequences for the physical and chemical properties of these structures.

Thin vanadium oxide layers have been deposited onto a clean Pd(111) surface by reactive evaporation of V metal in an oxygen atmosphere ($p_{O_2} = 2 \times 10^{-7}$ mbar, 250 °C substrate temperature [6]). The STM measurements were performed with a variable-temperature STM instrument (Oxford Instruments) [7] at room temperature. The DFT calculations were performed with the Vienna *ab initio* simulation package (VASP) [8] using the projector augmented wave method in the implementation of Kresse and Joubert [9]. The technical parameters are identical to those in Ref. [7] (see [10]).

Figure 1 shows an STM image of the surface formed after deposition of 0.9 monolayer equivalent (MLE) vanadium oxide [11] onto Pd(111). Several oxide phases are recognized, along with some bare Pd(111) areas. The first oxide layer at the Pd interface (surface V_2O_3 , *s*- V_2O_3) forms a (2×2) honeycomb structure (see inset A), which consists of two V atoms per unit cell located in the fcc and hcp hollow sites of the Pd(111) surface and three oxygen atoms in V-V bridge sites above two V atoms, thus forming a monolayer with a formal V_2O_3 stoichiometry as determined by STM and DFT calculations [7]. Note that the V atoms in the *s*- V_2O_3 layer are at the interface to the Pd(111). Besides the *s*- V_2O_3 phase two other vanadium oxide phases are recognized, which are distinguished by their different apparent heights in the STM. They are related to a VO_2 stoichiometry (V^{4+} oxidation state) on the basis of their V $2p$ core level signature. The V $2p_{3/2}$ core level XPS spectrum of this surface is shown in inset B and demonstrates the coexistence of two spectral components at 516.3 and 514.2 eV binding energy, which are associated with the VO_2 and *s*- V_2O_3 oxide phases, respectively [6,12]. The two coexistent VO_2 phases are also distinguished by their symmetries: a hexagonal (VO_2 -hex) and a rectangular (VO_2 -rect).

Image 2(a) shows three domains of the rectangular VO_2 -rect, while Fig. 2(b) displays the hexagonal VO_2 -hex oxide. Between the VO_2 oxide domains, the surface is covered with the *s*- V_2O_3 (2×2) structure as seen in both images. The VO_2 -rect phase [Fig. 2(a)] grows

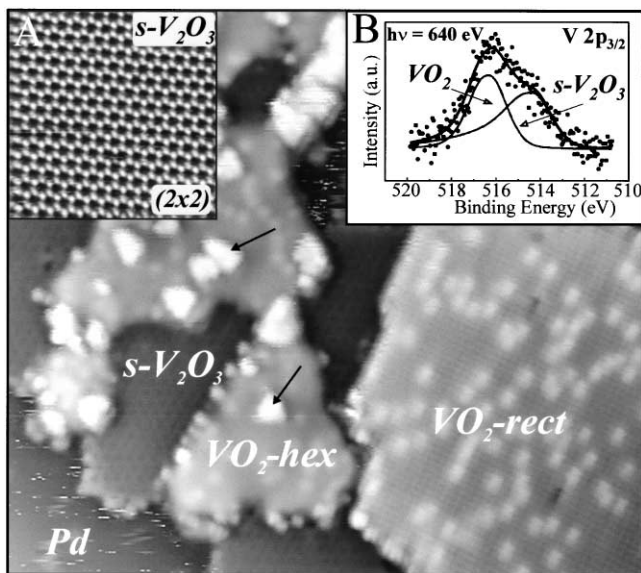


FIG. 1. STM image of 0.9 MLE vanadium oxide on Pd(111) ($300 \text{ \AA} \times 266 \text{ \AA}$; bias voltage: 1.0 V; tunneling current: 0.1 nA). Inset A shows a high-resolution image of the so-called surface- V_2O_3 ($s\text{-V}_2\text{O}_3$) phase. Inset B shows a V $2p_{3/2}$ core level XPS spectrum of 0.9 MLE V-oxide/Pd(111).

as well-ordered flat rectangular islands; the rows of maxima are separated by $\sim 3.8 \text{ \AA}$ and are misaligned by $\sim 7.5^\circ$ with respect to the $\langle 1\bar{1}0 \rangle$ crystallographic Pd(111) directions. Domain II is inclined by 15° with respect to domain I, and III is rotated by 120° . The surface unit cell dimensions of the $\text{VO}_2\text{-rect}$ phase are determined from the atomic-resolution STM image [inset of image 2(a)] to $a = 3.0 \text{ \AA}$, $b = 3.8 \text{ \AA}$. This evaluation of the STM image is confirmed by the LEED pattern of Fig. 2(c). The LEED pattern also contains the (2×2) reflections of the coexisting $s\text{-V}_2\text{O}_3$ structure. Although the $\text{VO}_2\text{-hex}$ phase is more difficult to image (corrugation $< 0.05 \text{ \AA}$) its atomic-scale hexagonal periodicity is recognizable in Fig. 2(b), and its unit cell vectors are determined to be $a = b = 2.80 \pm 0.05 \text{ \AA}$. This is very close to the unit cell vectors of the Pd(111) surface (2.75 \AA) and suggests a commensurate (1×1) overlayer lattice.

The DFT calculations establish that two unsupported V oxide thin-layer structures with a formal VO_2 stoichiometry are conceivable; a rectangular one and a hexagonal one with relaxed surface lattice parameters of $a = 2.96 \text{ \AA}$, $b = 3.71 \text{ \AA}$, and $a = b = 2.87 \text{ \AA}$, respectively. The rectangular is somewhat more stable than the hexagonal (energy of formation $E_{\text{form}} = -2.34 \text{ eV}$ versus -2.25 eV), but the small energy difference may not be sufficient to overcome kinetic limitations: the formation of $\text{VO}_2\text{-hex}$ requires only a local reordering of the already existing hexagonal V_2O_3 phase, whereas the formation of $\text{VO}_2\text{-rect}$ is linked to a long range reconstruction from a hexagonal to a rectangular phase. The calculated lattice constants are in very close agreement with the experimental ones, and we associate therefore the two VO_2 structures observed by STM with the DFT structural models shown in Figs. 2(d)

and 2(e). The center inset of Fig. 2(a) shows an STM simulation [7] of the model 2(d), which agrees well with the experimental image thus substantiating the structural model. The VO_2 layers in these models are oxygen terminated on both sides, which means that, according to DFT, the interface to the substrate transforms from Pd-V in the $s\text{-V}_2\text{O}_3$ phase to Pd-O-V. The binding energy between the oxide and the metal substrate is calculated to be around 400, 240, and 100 meV, if the interfacial oxygen atoms are located above top, bridge, and hollow sites, respectively.

An interesting aspect of the $\text{VO}_2\text{-rect}$ phase is its orientation with respect to the Pd(111) surface. This orientation becomes plausible if one realizes that the diagonals of the rectangular reciprocal unit cells coincide with the Pd(111) reciprocal unit cell vectors [see LEED pattern, Fig. 2(c)]. Thus, a row matching condition [13] is achieved with the observed rotational angle of 7.5° with respect to the $\langle 1\bar{1}0 \rangle$ directions, as illustrated in Fig. 2(f). By means of the matching, the oxygen atoms at the Pd- $\text{VO}_2\text{-rect}$ interface avoid the Pd-hollow sites, which are particularly unfavorable. Hence, the row matching of the overlayer with the substrate lowers the interfacial energy.

The $\text{VO}_2\text{-rect}$ phase collapses on further V oxide deposition and the growth of additional oxide layers commences on top of the $\text{VO}_2\text{-hex}$ phase, converging gradually to a V_2O_3 bulklike phase. The initial growth on top of $\text{VO}_2\text{-hex}$ is in the form of small triangular islands [see arrows in Fig. 1(a)]. In Fig. 3(a), the $\text{VO}_2\text{-hex}$ phase is visible with the grey contrast and no apparent corrugation, but the periodicity of the hexagonal overlayer on top of it (brighter contrast) is clearly recognized. This image reveals that the growth of the next V oxide layer on top of the $\text{VO}_2\text{-hex}$ phase has twice the periodicity of the $\text{VO}_2\text{-hex}$ layer, i.e., it is also a (2×2) overlayer. As demonstrated by the DFT calculations, a V_2O_3 -type (2×2) overlayer with a similar structure as surface- V_2O_3 stabilizes the $\text{VO}_2\text{-hex}$ phase. The inset in Fig. 3(a) shows a simulated STM image of such a V_2O_3 -type overlayer on a $\text{VO}_2\text{-hex}$ film (overall V_6O_{11} layer). The simulation is in good agreement with the STM image and strongly supports the model.

This (2×2) structure is a precursor phase to bulk-type V_2O_3 , which is fully developed for oxide coverages > 3 MLE [Fig. 3(b)]. This shows terraces separated by a step height of 2.3 \AA in accord with the V_2O_3 crystal structure [14]. The V $2p_{3/2}$ XPS spectrum of this surface (not shown) contains a single peak at $\sim 515.5 \text{ eV}$ binding energy confirming the V_2O_3 stoichiometry [6]. The hexagonal V_2O_3 surface unit cell (lattice parameter $a = 4.91 \text{ \AA}$) is aligned along the $\langle 1\bar{2}1 \rangle$ directions [see Fig. 3(b)], and the unit cell is thus rotated by 30° with respect to the Pd(111) substrate unit cell vectors. Note the mismatch between the V_2O_3 bulk lattice and the $\sqrt{3}$ direction of Pd(111) is only 3.7%. There is also excellent lattice matching between the V_2O_3 bulk structure and the $\sqrt{3}$ directions of the $\text{VO}_2\text{-hex}$ phase (4.91 versus 4.93 \AA). This close lattice match is the reason that the $\text{VO}_2\text{-hex}$ phase is involved in mediating further oxide layer growth. The bulk-type V_2O_3 phase has

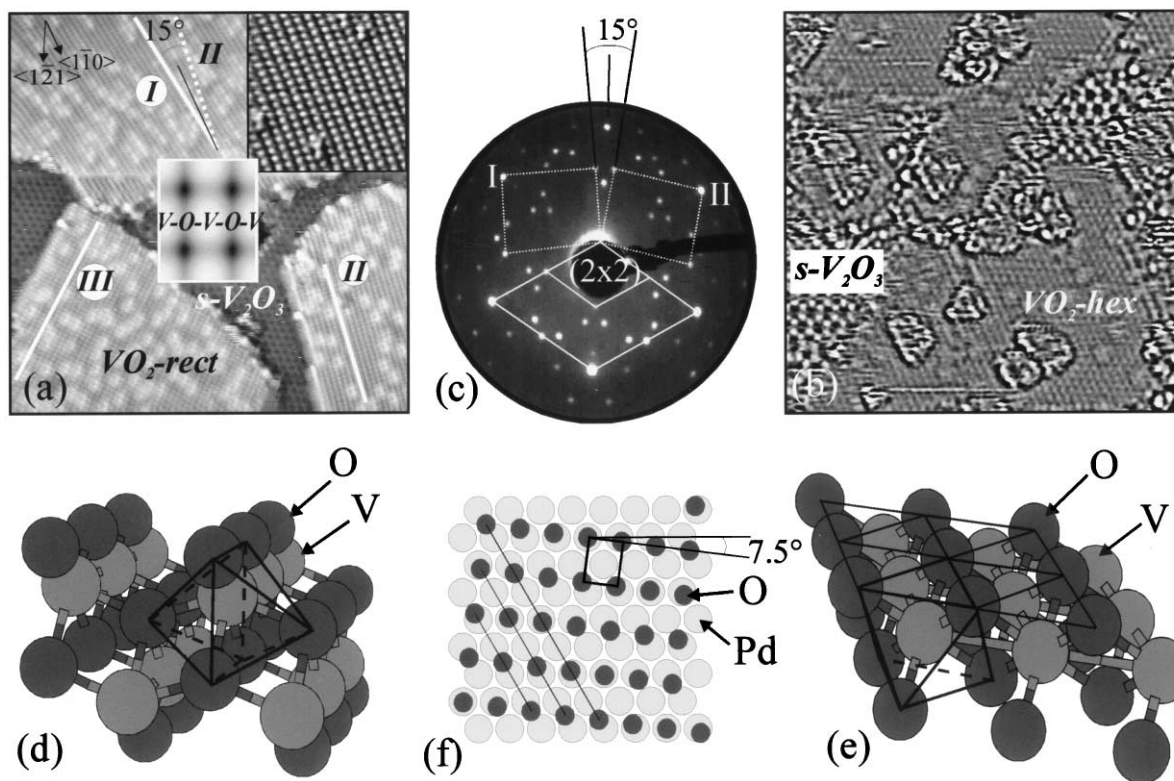


FIG. 2. (a) STM image ($275 \text{ \AA} \times 275 \text{ \AA}$; 0.5 V, 1.0 nA) of 1 MLE V oxide on Pd(111). The upper-right inset is a high-resolution STM image, the center inset a theoretical simulation. The theoretical calculations reveal that the V atoms, although below the O atoms, are imaged as protrusion in the STM. (b) STM image ($133 \text{ \AA} \times 133 \text{ \AA}$; 0.6 V, 0.5 nA) of the VO_2 -hex phase. (c) LEED pattern of the 1 MLE V-oxide/Pd(111) surface. (d) Structural model of the VO_2 -rect phase. (e) Structural model of the VO_2 -hex phase. (f) Model of the orientation of the VO_2 -rect unit cell on the Pd(111) surface, revealing row matching.

the (0001) face of the corundum lattice parallel to the substrate plane and its termination, calculated for the oxygen chemical potentials (pressures) considered in the present experiment, is by O-V dimers, i.e., O-V-O V_2O_3 in terms of layers [see lower inset of Fig. 3(b)]. The corresponding STM simulation [upper inset in Fig. 3(b)] agrees well with the experimental image.

The physical origin of the layer-dependent evolution of vanadium oxide structures on Pd(111) is underpinned by the DFT analysis. In Fig. 4 we show the change of the surface energy ΔE_{surf} upon adsorption of vanadium and oxygen [15]:

$$\Delta E_{\text{surf}} = E_{\text{slab}} - E_{\text{clean-slab}} - \mu_{\text{O}}N_{\text{O}} - \mu_{\text{V}}N_{\text{V}}.$$

For oxygen, we assume a chemical potential corresponding roughly to the experimental conditions under consideration ($\mu_{\text{O}} = -2.0 \text{ eV}$ with respect to a free O_2 dimer), and we set the chemical potential of vanadium to $\mu_{\text{V}} = [5E(\text{V}_2\text{O}_3) - 3\mu_{\text{O}}]/2$. Only phases which lie below lines connecting any other two phases are stable, and it is easily recognized that a change of μ_{V} will not affect the stability considerations. At low coverage, $s\text{-V}_2\text{O}_3$ with V atoms at the Pd interface is the most stable structure, and it covers the entire surface at a coverage of 0.5 ML. Growth of additional adlayers on this structure is not favored, since it derives its stability from a pseudogap at the Fermi level, which is destroyed

by the bonding to additional layers. Therefore even the most favorable continuation on top of surface- V_2O_3 , a monolayer of bulk- V_2O_3 ($s\text{-V}_2\text{O}_3/\text{bulk-V}_2\text{O}_3$), is unstable, and a transition to one of the two thin VO_2 films lowers the surface energy significantly. The DFT predicts only one thermodynamically stable film, VO_2 -rect, but, as already mentioned, kinetics might well lead to the observed patches of VO_2 -hex. Further oxide growth on VO_2 -rect is unfavorable, but VO_2 -hex becomes stabilized by an adlayer that is similar in structure to $s\text{-V}_2\text{O}_3$ ($4\text{VO}_2\text{-hex}/s\text{-V}_2\text{O}_3$) [15]. DFT indicates that neither the rectangular nor the hexagonal film can directly participate in further growth, but the hexagonal $4\text{VO}_2\text{-hex}/s\text{-V}_2\text{O}_3$ structure probably favors the formation of structures with similar lattice parameters and symmetry. Also energetic arguments alone ultimately lead to the formation of the bulk- V_2O_3 corundum phase ($\text{O}_3 + n\text{V}_2\text{O}_3 + \text{VO}$), with oxygen at the interface on top of Pd sites.

It is remarkable that the oxidation state of vanadium is initially 3^+ , then increases to 4^+ , and finally becomes 3^+ again. We first note that the thermodynamically stable bulk phase under the present experimental conditions is VO_2 [15]. The formation of stable thin films with such a stoichiometry is therefore not astonishing; however, it is emphasized that the observed and predicted structures differ completely from that of bulk- VO_2 . The transformation from the thin film structures to bulk- V_2O_3 occurs

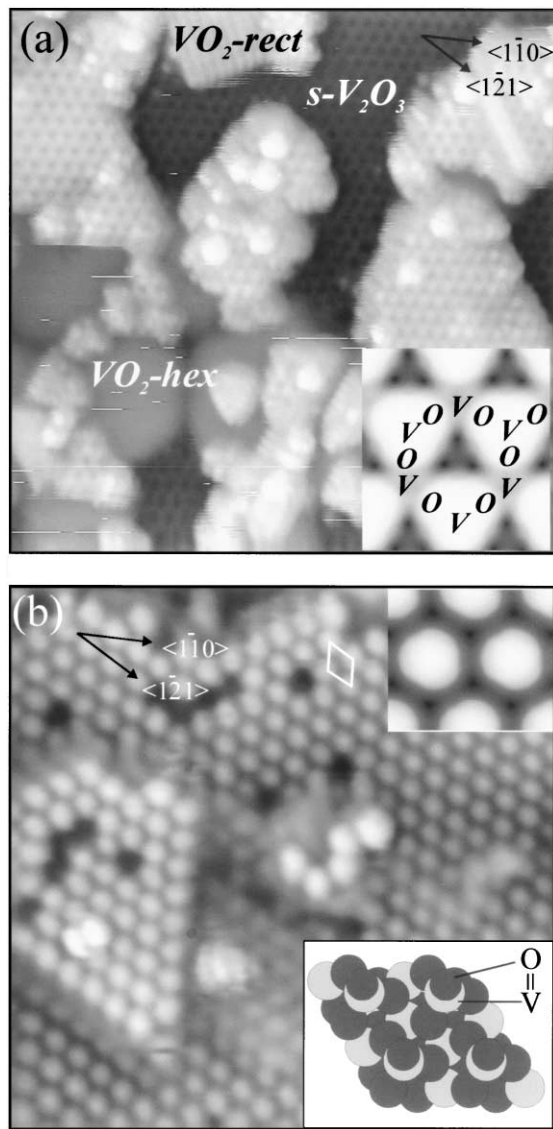


FIG. 3. (a) STM image ($200 \text{ \AA} \times 200 \text{ \AA}$; 0.7 V, 1.0 nA) of 1.3 MLE V oxide on Pd(111); inset is a STM simulation of a V_6O_{11} layer. (b) STM image ($100 \text{ \AA} \times 100 \text{ \AA}$; -0.3 V, 0.1 nA) of 3 MLE V oxide on Pd(111) showing the bulk-type V_2O_3 phase. The insets show a structural model and a STM simulation of the O-V-O₃V₂O₃ termination of bulk V_2O_3 .

approximately at 3–4 layers, where the formal stoichiometry is again approximately 1V:2O ($O_3 + 3V_2O_3 + VO = V_7O_{13}$). At this point, the metal-oxide interface energy is sufficient to stabilize V_2O_{3+x} compared to bulk- VO_2 .

In summary, a sequence of novel vanadium oxide phases with different structures and oscillating oxidation states has been detected in ultrathin layers at the interface between a Pd(111) surface and a vanadium oxide thin film. These interface-mediated structures are metastable with respect to increasing oxide thin film growth and transform into a stable oxide configuration only for films exceeding a critical thickness (>3 MLE oxide coverage in the present V-oxide/Pd(111) case, corresponding to $>4.5V_2O_3$ lay-

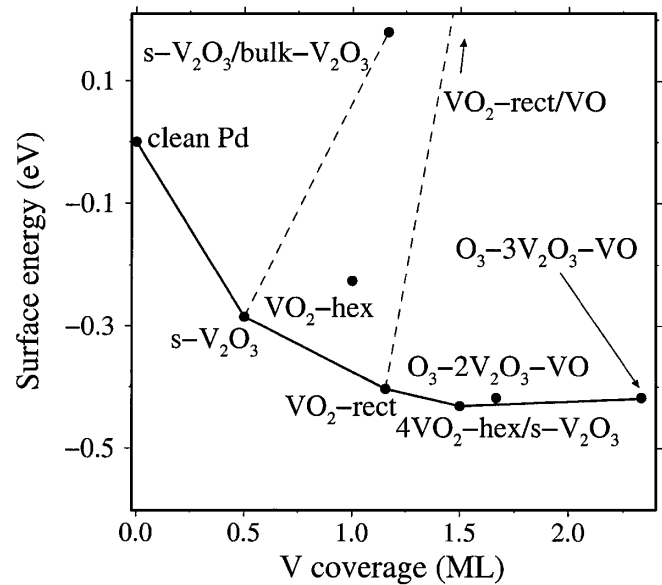


FIG. 4. Change of surface energy on deposition of vanadium and oxygen on Pd(111) versus the vanadium coverage.

ers). An important aspect demonstrated in this study is that bulk oxide structures are of little relevance for oxide growth at the interface to a dissimilar material. We believe that similar metastable phases may occur generally in the early stages of the formation of thin oxide layers. Their influence on the physiochemical properties of ultrathin oxide systems may be important for the technological applications of these systems.

Research was supported by the Austrian Science Foundation.

- [1] S. A. Chambers, Surf. Sci. Rep. **39**, 105 (2000).
- [2] R. Franchy, Surf. Sci. Rep. **38**, 195 (2000).
- [3] G. C. Bond and S. F. Tahir, Appl. Catal. **71**, 1 (1991).
- [4] G. Centi, Appl. Catal. A **147**, 267 (1996).
- [5] C. Noguera, J. Phys. Condens. Matter **12**, R367 (2000).
- [6] F. P. Leisenberger *et al.*, J. Vac. Sci. Technol. A **17**, 1743 (1999).
- [7] S. Surnev *et al.*, Phys. Rev. B **61**, 13 945 (2000).
- [8] G. Kresse and J. Furthmüller, Phys. Rev. B **54**, 11 169 (1996).
- [9] G. Kresse and D. Joubert, Phys. Rev. B **59**, 1758 (1999).
- [10] The technical errors (unregarded DFT related errors) in the reported energies are of the order of 20 meV.
- [11] The actual oxide surface coverage depends on both the morphology and the stoichiometry of the oxide layer. We therefore use the term *monolayer equivalents*, i.e., the evaporated amount of V as determined by a quartz microbalance and referred to the density of Pd(111) surface atoms, to indicate the relative oxide coverage.
- [12] G. A. Sawatzky and D. Post, Phys. Rev. B **20**, 1546 (1979).
- [13] H. H. Weitering *et al.*, Phys. Rev. B **45**, 5991 (1992).
- [14] P. D. Dernier, J. Phys. Chem. Solids **31**, 2569 (1970).
- [15] G. Kresse *et al.* (to be published).